Inorg. Chem. **2004**, *43*, 2762–2764

$APSe_6$ (A = K, Rb, and Cs): Polymeric Selenophosphates with Reversible Phase-Change Properties

In Chung, Junghwan Do, Christian G. Canlas, David P. Weliky,* and Mercouri G. Kanatzidis*

Department of Chemistry, Michigan State University, East Lansing, Michigan 48824

Received December 17, 2003

The ternary alkali selenophosphates $KPSe_6$ and $RbPSe_6$ crystallize in the polar orthorhombic space group $Pca2_1$ with $a = 11.7764(17)$ Å, $b = 6.8580(10)$ Å, $c = 11.4596(16)$ Å, and $Z = 4$ for $RbPSe_6$. $CsPSe_6$ crystallizes in the monoclinic space group $P2/n$ with $a = 6.877(3)$ Å, $b = 12.713(4)$ Å, $c = 11.242(4)$ Å, $\beta = 92.735(7)°$, and $Z = 4$. All compounds feature the one-dimensional infinite chain of $[PSe_2(Se)_4^-]$, where each P atom is connected with Se_4^{2-} bridge. These compounds show reversible glass–crystal transition, and ^{31}P NMR data suggest that crystallization and infinite $[PSe_6^-]$ chain formation are coupled processes.

Because complex metal chalcophosphates form readily in an alkali chalcogenide flux environment,[1] it is important to know more about what species are present during these reaction conditions. A number of free chalcophosphate anionic ligands $[P_xQ_y]^{n-}$ (Q = S, Se) have been isolated and characterized as alkali metal salts, including $[PQ_4]^{3-}$,[2] $[PSe_4]^{3-}\cdot 2Se_6$,[3] $[P_2S_6]^{2-}$,[4] $[P_2Q_6]^{4-}$,[5] $[P_2Se_9]^{2-}$,[6] $[P_8Se_{18}]^{6-}$,[7] and $[P_2S_{10}]^{4-}$.[8] They are all discrete molecular anions mainly as they do not coordinate to metals in the structure. Investigations of new $[P_xQ_y]^{n-}$ building blocks could help us understand the stability ranges of these in the flux and how the observed solid-state structure motifs arise.[9] The alkali salts of $[P_xQ_y]^{n-}$ (Q = S, Se) can also be useful starting materials for solid-state reactions or coordination chemistry in solution.

Here we report on the isolation of a new polymeric $[PSe_6^-]$ anion crystallized as alkali salts $APSe_6$ (A = K, Rb, and Cs). These materials undergo an interesting reversible crystal−glass transition.[10]

$KPSe_6$ (**1**) and $RbPSe_6$ (**2**) are isostructural and adopt the polar space group $Pca2_1$. This discussion will concentrate mainly on the Rb^+ salt[11] which consists of infinite one-dimensional chains of $^1_\infty[PSe_6^-]$ along the *a*-axis and separated by Rb^+ ions, Figure 1a. The crystallographically unique anion has PSe_4 tetrahedra condensed with diselenide linkages to give the polymeric $^1_\infty[PSe_6^-]$ chain. The PSe_4 tetrahedron is only slightly distorted from the ideal one with the Se−P−Se angles ranging from 101.46(7)° to 119.79(8)°. The P−Se distances are normal at 2.1529(18)−2.2994(17) Å. The Se−Se distances range from 2.3534(10) to 2.3859(10) Å. The dihedral angles around the bonds Se(1)−Se(2), Se(2)−Se(3), and Se(3)−Se(4) are −93.53(5)°, 112.41(4)°, and 87.35(5)°. The largest deviation from 90° gives the longest internal Se(2)−Se(3) distance as reported for disulfides[12] and leads to a bond distance alternation in the Se_4^{2-} unit. This trend is generally shown in unligated Se_4^{2-} ions.[13] Unusually short Se···Se nonbonding interactions between adjacent chains along the *c*-axis are observed at 3.217(1)−3.350 (1) Å. Short intra- and interlayer Se···Se interactions, much shorter in distance than the van der Waals radii sum of 3.80 Å,[14] play a crucial role in

* To whom correspondence should be addressed. E-mail: kanatzid@cem.msu.edu (M.G.K.); weliky@cem.msu.edu (D.P.W.).

(1) Kanatzidis, M. G. *Curr. Opin. Solid State Mater. Sci*. **1997**, *2*, 139.
(2) (a) Mercier, R.; Malugani, J.-P.; Fahys, B.; Robert, G. *Acta Crystallogr., Sect. B* **1982**, *38*, 1887. (b) Schäfer, H.; Schäfer, G.; Weiss, A. *Z. Naturforsch., B: Anorg. Chem. Org. Chem.* **1965**, *20*, 811. (c) Jansen, M.; Henseler, U. *J. Solid State Chem.* **1992**, *99*, 110.
(3) Dickerson, C. A.; Fisher, M. J.; Sykora, R. E.; Albrecht-Schmitt, T. E.; Cody, J. A. *Inorg. Chem.* **2002**, *41*, 640
(4) Brockner, W.; Becker, R.; Eisenmann, B.; Schäfer, H. *Z. Anorg. Allg. Chem.* **1985**, *520*, 51.
(5) Mercier, R.; Malugani, J.-P.; Fahys, B.; Douglade, J.; Robert, G. *J. Solid State. Chem.* **1982**, *43*, 151.
(6) Chondroudis, K.; Kanatzidis, M. G. *Inorg. Chem*. **1995**, *34*, 5401.
(7) Chondroudis, K.; Kanatzidis, M. G. *Inorg. Chem*. **1998**, *37*, 2582.
(8) Aitken, J. A.; Canlas, C.; Weliky, D. P.; Kanatzidis, M. G. *Inorg. Chem*. **2001**, *40*, 6496.
(9) Canlas, C. G.; Kanatzidis, M. G.; Weliky, D. P. *Inorg. Chem*. **2003**, *42*, 3399.
(10) Pure $APSe_6$ (A = K, Rb, and Cs) was achieved by a stoichiometric mixture of $A_2Se/P_2Se_5/Se = 1/1/6$ under vacuum in a silica tube at 350 °C for 10 days. Energy dispersive spectroscopy analysis of the crystals showed an average composition of "$KPSe_{6.2}$", "$Rb_{1.2}PSe_{6.1}$", and "$CsPSe_{6.2}$", respectively, for the orange rod-type single crystals. The glassy phase of $APSe_6$ was prepared from a stoichiometric mixture of $A_2Se/P_2Se_5/Se = 1/1/6$ under vacuum in a quartz tube at 800−900 °C for 1−2 min and subsequent quenching to room temperature. All compounds are air-sensitive and begin to decompose in a week and are unstable under *N*,*N*-dimethylformamide and H_2O but relatively stable under acetonitrile.
(11) Crystal data for $RbPSe_6$ at 293(2) K: Siemens SMART Platform CCD diffractometer, Mo Kα radiation ($\lambda = 0.71073$ Å), $Pca2_1$, $a = 11.7764(17)$ Å, $b = 6.8580(10)$ Å, $c = 11.4596(16)$ Å, $V = 925.5(2)$ Å^3, $Z = 4$, $D_c = 4.236$ g/cm^3, crystal dimensions $0.028 \times 0.167 \times 0.037$ mm^3, $\mu = 29.031$ mm^{-1}, $2\theta = 2.97-28.32°$, 8770 total reflections, 2193 unique reflections with $R(\text{int}) = 0.047$, refinement on F^2, GOF = 0.977, 73 parameters, $R_1 = 2.59\%$, $wR_2 = 4.99\%$ for $I > 2\sigma(I)$. An empirical absorption correction was done using SADABS, and all atoms were refined anisotropically. Structure solution and refinement were performed with SHELXTL.
(12) Hordvik, A. *Acta Chem. Scand*. **1966**, *20*, 1885.
(13) Brese, N. E.; Randall, C. R.; Ibers, J. A. *Inorg. Chem*. **1988**, *27*, 940.

10.1021/ic035448q CCC: $27.50
Published on Web 04/03/2004

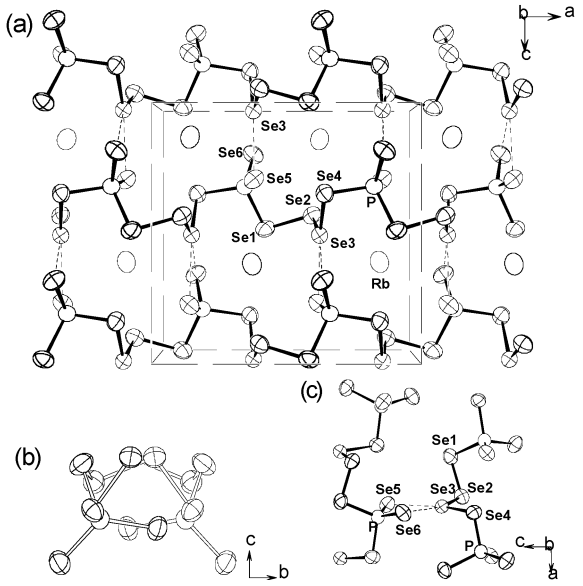

Figure 1. (a) Structure of $RbPSe_6$ viewed down the *b*-axis. The Rb^+ ions are coordinated by 12 Se atoms from four selenophosphate chains. Selected bond distances (Å): P−Se(1), 2.2994(17); P−Se(4), 2.2521(19); P−Se(5), 2.1529(18); P−Se(6), 2.1530(17); Se(1)−Se(2), 2.3473(10); Se(2)−Se(3), 2.3859(10); Se(3)−Se(4), 2.3534(10). Selected bond angles (deg): Se(1)−P−Se(4), 104.41(7); Se(1)−P−Se(5), 108.49(7); Se(1)−P−Se(6), 111.19(8); Se(4)−P−Se(5), 110.30(8); Se(4)−P−Se(6), 101.46(7); Se(5)−P−Se(6), 119.79(8); Se(1)−Se(2)−Se(3), 101.27(3); Se(2)−Se(3)−Se(4), 103.92(4). Dashed lines indicate weak Se···Se interactions (Å): Se(3)···Se(5), 3.350(1); Se(3)···Se(6), 3.217(1). (b) View of a $^1_\infty[PSe_6^-]$ chain looking down the *a*-axis, clearly showing its polar character. (c) Segment of the $^1_\infty[PSe_6^-]$ anion showing the short Se···Se interactions. The thermal ellipsoids with 90% probability are shown.

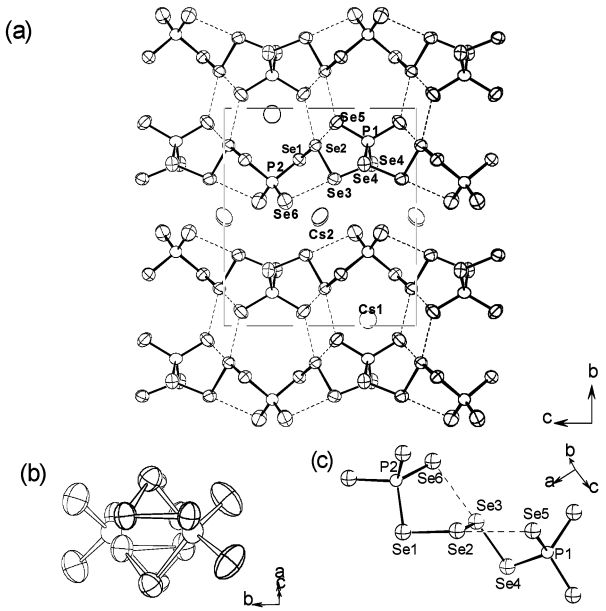

Figure 2. (a) Structure of $CsPSe_6$ viewed down the *a*-axis. Both Cs(1) and Cs(2) are surrounded by four different $[PSe_6^-]$ chains. Selected bond distances (Å): P(1)−Se(4), 2.240(2); P(1)−Se(5), 2.135(2); P(2)−Se(1), 2.262(2); P(2)−Se(6), 2.138(2); Se(1)−Se(2), 2.3549(16); Se(2)−Se(3), 2.3798(15); Se(3)−Se(4), 2.3558(16). Selected bond angles (deg): Se(4)−P(1)−Se(4), 108.43(15); Se(5)−P(1)−Se(5), 117.54(17); Se(1)−P(2)−Se-(6), 102.95(5); Se(6)−P(2)−Se(6), 117.92(17); Se(1)−Se(2)−Se(3), 100.20-(5); Se(2)−Se(3)−Se(4), 98.20(5); P(1)−Se(4)−Se(3), 98.56(5); P(2)−Se(1)−Se(2), 97.81(6). Dashed lines indicate weak Se···Se interactions (Å): Se(2)···Se(5), 3.280(7); Se(3)···Se(6), 3.160(2); Se(2)···Se(5′), 3.248-(2). (b) View of a $^1_\infty[PSe_6^-]$ chain looking down $[10\bar{1}]$ axis. (c) Local geometry of the $^1_\infty[PSe_6^-]$ anion in $CsPSe_6$ showing the short Se···Se interactions. The thermal ellipsoids with 90% probability are shown.

influencing the crystal structure. In fact, other low-dimensional compounds such as $NbSe_3$ with its charge density wave phenomenon exhibit similar Se···Se interactions of 3.30 Å.[15] In K_2Se_5,[16] short contacts between the Se_5^{2-} ions are also observed. The shorter Se···Se interactions in **2** affect the local geometry of the $^1_\infty[PSe_6^-]$ chains to form pseudo-lamellar packing and relatively long Se−Se bonds due to the delocalization of electrons through short Se···Se contacts, Figure 1c.

$CsPSe_6$ (**3**)[17] is a centrosymmetric compound also with $^1_\infty[PSe_6^-]$ chains but of a different conformation than in the K^+ and Rb^+ analogues, Figure 2a. The differences in conformation are seen clearly in projection of the two chains in Figure 1b and 2b. Adjacent $^1_\infty[PSe_6^-]$ chains along *b*-axis are related by a 2-fold symmetry operation along the *a*-axis. P−Se distances range from 2.135(2) to 2.262(2) Å. The Se−Se distances with alteration are similar to the Rb^+ analogue at 2.3549(16)−2.3798(15) Å. The dihedral angle around the Se(2)−Se(3) bond of −121.06(1)° contributes to its longer distance than the external ones. Short Se···Se interactions are observed at 3.160(2)−3.280(7) Å, even shorter than those of **2**. Interchain interactions generate a pseudo-lamellar packing and influence the conformation of the Se_4^{2-} linkage to form straight lines of Se(1)−Se(2)···Se(5) and Se(4)−Se(3)···Se(6) connections and possibly maximize the pπ orbital overlap, Figure 2c.

The $[PSe_2(Se_4)^-]$ anion is a rare example of a free-standing polymeric chalcophosphate with no coordinating metals. The only other reported polymeric anion is the $^1_\infty[P_3Se_4^-]$ ion which was found bound to Ru or Os atoms in $K_3RuP_5Se_{10}$,[18] $Rb_3RuP_5Se_{10}$, $A_3OsP_5Se_{10}$ (A = K, Rb).[19]

According to differential thermal analysis (DTA) performed at a rate of 10 °C/min, $RbPSe_6$ (**2**)[20] and $CsPSe_6$ (**3**) melt congruently at 315 and 303 °C, respectively, (Figure

(14) Bond, A. *J. Phys. Chem.* **1964**, *68*, 441.
(15) (a) *Electronic Properties of Inorganic Quasi-One-Dimensional Compounds, Part II*; Monceau, P., Ed.; D. Reidel Publishing Company: Dordrecht, 1985. (b) Canadell, E.; Rachidi, E.-I.; Pouget, J. P.; Gressier, P.; Meerschaut, A.; Rouxel, J.; Jung, D.; Evain, M.; Whangbo, M.-H. *Inorg. Chem.* **1990**, *29*, 1401.
(16) Mueller, V.; Frenzen, G.; Dehnicke, K.; Fenske, D. *Z. Naturforsch., B: Chem. Sci.* **1992**, *47*, 205.
(17) Crystal data for $CsPSe_6$ at 296(2) K: Siemens SMART CCD diffractometer, Mo Kα radiation (λ = 0.71073 Å), *P2/n*, a = 6.877-(3) Å, b = 12.713(4) Å, c = 11.242(4) Å, β = 92.735(7)°, V = 981.8-(6) Å^3, Z = 4, D_c = 4.236 g/cm^3, crystal dimensions 0.139 × 0.014 × 0.014 mm^3, μ = 26.095 mm^{-1}, 2θ = 1.60−28.32°, 5747 total reflections, 2260 unique reflections with R(int) = 0.0535, refinement on F^2, GOF = 1.024, 79 parameters, R_1 = 3.81%, wR_2 = 8.74% for $I > 2\sigma(I)$. Cs(2) was originally assigned to special position (0, 0.5, −0.5), but because of a large *x*-axis atomic displacement parameter (U_{11}, U_{22}, U_{33}) = (0.1015, 0.0487, 0.0208), it was allowed into a general position. This refined to (−0.972682, 0.494929, −0.501068) with reasonable displacement parameters of (U_{11}, U_{22}, U_{33}) = (0.0559, 0.0489, 0.0211). Cs(2), however, still exhibited disorder near its refined position leading to relatively high standard deviation of bond lengths between Cs(2) and P and Se atoms. An empirical absorption correction was done using SADABS, and all atoms were refined anisotropically.
(18) Chondroudis, K.; Kanatzidis, M. G. *Angew. Chem., Int. Ed. Engl.* **1997**, *36*, 1324.
(19) Chung, I.; Kanatzidis, M. G. Unpublished results. $Rb_3RuP_5Se_{10}$, $K_3OsP_5Se_{10}$, and $Rb_3OsP_5Se_{10}$ are isostructural to $K_3RuP_5Se_{10}$.

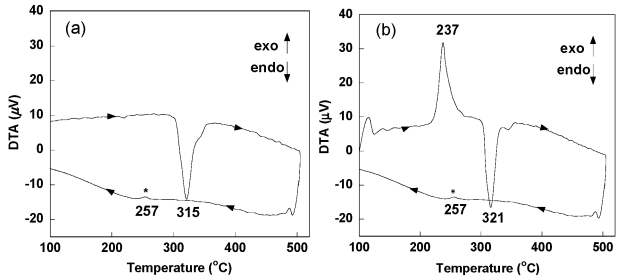

Figure 3. Differential thermal analysis diagrams of $RbPSe_6$ representing (a) melting in the first cycle with no crystallization upon cooling and (b) subsequent recrystallization and complete melting upon heating in the second cycle. Asterisks indicate the vitrification upon cooling.

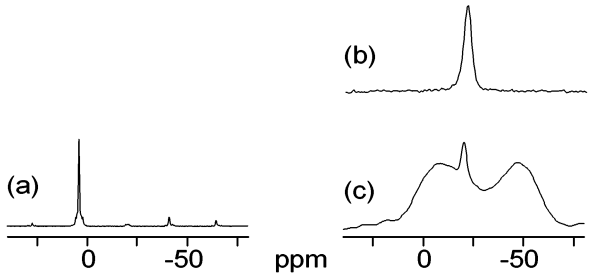

Figure 4. ^{31}P NMR spectra of $RbPSe_6$ taken at 161.5 MHz Larmor frequency. Spectra a and c are for the crystalline and glassy materials, respectively, and were obtained at ambient temperature and with MAS frequency of ~11 kHz. Spectrum b is for the melt at 350 °C and was obtained under static conditions. For glassy $RbPSe_6$, $m = \pm 1$ spinning sidebands are seen in a spectrum with a larger range of displayed shifts.

3) and form dark red glasses rather than crystals upon cooling.[21] Crystallization is only achieved on heating. The glasses recrystallize exothermically at 237 °C for **2** and 206 °C for **3** upon subsequent heating followed by melting at 321 and 310 °C for **2** and for **3**, respectively. $RbPSe_6$ showed vitrification at 257 °C on cooling to room temperature. The XRD patterns after recrystallization are the same as those of pristine **2** and **3** indicating full recovery of the original crystal structure. Recrystallization and vitrification are reversible as they were repeatedly observed by repeating the DTA cycles. We may speculate that the facile crystallization of these glasses suggests that the glass structure is somewhat related to the crystal structure, and given the polar character of the Rb salt, we may expect a similar polar nature for the precursor glass.

The solid-state diffuse reflectance UV−vis spectra of both crystalline and glassy $APSe_6$ (A = K, Rb, and Cs) reveal sharp absorption edges. The band gaps of crystalline phases **1**, **2**, and **3** revealed 2.16, 2.18, and 2.16 eV values while those of glassy counterparts **4**, **5**, and **6** showed 1.82, 1.91, and 1.71 eV values, respectively, which are consistent with their respective orange and dark red colors. It is noteworthy that red shifts in the absorption edge are typical in glassy phases. Glass formation in compounds with extended solid-state structures generally produces massive defects and mid-gap states, which leads to lower band gaps than corresponding crystalline phases.[22] This phenomenon is a key aspect of optical storage systems based on phase-change materials.[23] Furthermore, the polar K^+ and Rb^+ salts enable them to be explored for nonlinear optical properties.

The far IR spectra of $RbPSe_6$ display absorption peaks at 482(s), 424(s), 386(s), 356(m), 247(m), 228(w), and 164(w) cm^{-1}. The peaks at 247 cm^{-1} are attributed to Se−Se stretching.[5,24] Those at higher energies are diagnostic of P−Se vibrations.[25] The far IR spectra of glassy $RbPSe_6$ display much broader and weaker peaks at 507(w), 420(w), 385(sh), and 252(sh) cm^{-1}. A comparison with crystalline $RbPSe_6$ suggests that the building block $[PSe_6^-]$ unit is substantially intact in the glass but lacks long-range order. The bridging Se_4^{2-} chains seem to be severely disordered in the glassy phase according to the very weak and broad Se−Se stretching vibrations.

^{31}P NMR provided further insight into bonding and structure (Figure 4). For crystalline $RbPSe_6$ under magic angle spinning (MAS), the major peak has an isotropic chemical shift of 4.3 ppm and a full-width at half-maximum (FWHM) line width of 0.5 ppm. This shift is ~40 ppm higher than a typical shift of $[P_2Se_9]^{4-}$, a comparable discrete unit with bridging Se.[9] In addition, for discrete selenophosphate units, the $\delta_{11}-\delta_{33}$ chemical shift anisotropy (CSA) principal value difference correlates inversely with the degree of local symmetry about P, with ~65 ppm values observed for discrete tetrahedral $[PSe_4]^{3-}$ units and ~200 ppm values observed for $[P_2Se_9]^{4-}$ units.[9] The ~115 ppm CSA value observed for $RbPSe_6$ fits within this correlation, with the pseudo-C_2 symmetry of P in $^1_\infty[PSe_6^-]$ chains intermediate between the high and low symmetries of P in $[PSe_4]^{3-}$ and $[P_2Se_9]^{4-}$ anions, respectively.

In a 350 °C melt, the static ^{31}P spectrum has a single resonance with −21 ppm peak chemical shift and 4 ppm fwhm line width. The shift is typical of PSe_4-type bonding,[9] and the narrow line width is diagnostic of rapidly tumbling small molecular species such as $[PSe_6]_m^{n-}$ ring-based molecules which would result from depolymerization of $^1_\infty[PSe_6^-]$ chains. In the $RbPSe_6$ glassy phase, there is a broad ^{31}P MAS signal centered at −25 ppm. The similarity of the average shifts of the melt and glass spectra and the broad width of the glass spectrum are consistent with a frozen melt model for the glass with associated conformational, packing, and possibly molecular heterogeneity. Overall, the NMR, crystallographic, and DTA data suggest that crystallization and $^1_\infty[PSe_6^-]$ chain formation are coupled processes.

Acknowledgment. Financial support was provided by the National Science Foundation (DMR-0127644).

Supporting Information Available: X-ray crystallographic file, in CIF format. This material is available free of charge via the Internet at http://pubs.acs.org.

IC035448Q

(20) The thermal behavior of $KPSe_6$ showed the same patterns as that of $RbPSe_6$.
(21) The powder X-ray diffraction (XRD) patterns after each DTA cycle showed that amorphous glasses had formed.
(22) Dhingra, S.; Kanatzidis, M. G. *Science* **1992**, *258*, 1769.
(23) (a) Feinlieb, J.; deNeufville, J. P.; Moss, S. C.; Ovshinsky, S. R. *Appl. Phys. Lett*. **1971**, *18*, 254. (b) Maeda, Y.; Andoh, H.; Ikuta, I.; Minemura, H. *J. Appl, Phys*. **1988**, *64*, 1715.
(24) Wachhold, M.; Kanatzidis, M. G. *J. Am. Chem. Soc*. **1999**, *121*, 1, 4189.
(25) Chondroudis, K.; Kanatzidis, M. G. *Chem. Commun*. **1996**, 1371.